2008

Theoretical Analysis of the Effect of Oil Atomization in the Cylinder of a Reciprocating Ammonia Compressor

Rodrigo Kremer
Federal University of Santa Catarina

Cesar J. Deschamps
Federal University of Santa Catarina

Jader R. Barbosa
Federal University of Santa Catarina

Theoretical Analysis of the Effect of Oil Atomization in the Cylinder of a Reciprocating Ammonia Compressor

Rodrigo KREMER, Cesar J. DESCHAMPS*, Jader R. BARBOSA Jr.

Department of Mechanical Engineering, Federal University of Santa Catarina,
88040-900, Florianopolis, SC, Brazil

* Corresponding Author
Phone/Fax: ++ 55 48 3234 5166, e-mail: deschamps@polo.ufsc.br

ABSTRACT

An analysis of the influence of oil atomization in the cylinder of a reciprocating compressor using ammonia as a refrigerant is presented. During compression, oil atomization enhances heat removal from the refrigerant vapor and, as a consequence, an overall temperature decrease is brought about in the compressor. The cooling effect of the compression process allows a reduction of losses associated with compression inefficiency. The simulation methodology adopted in the analysis is based on an integral control volume formulation for mass and energy conservation. Computational Fluid Dynamics (CFD) simulations using commercial software were also performed to support some required data for the theoretical analysis. The effect of oil atomization on compression performance is presented and discussed based on oil injection parameters, such as nozzle positioning, oil temperature and flow rate.

1. INTRODUCTION

In ammonia refrigeration compressors, a significant portion of the energy losses is due to refrigerant superheating along the suction path inside the compressor and during vapor compression itself. The high levels of superheat resulting from the compression of ammonia cause a reduction of the volumetric efficiency and of the refrigerant mass flow rate and an increase in the compression work per unit mass (Gosney, 1982). In addition, the high discharge temperatures typical of ammonia compressors may present serious reliability issues in the case of high pressure ratio applications. Figure 1 illustrates the increase in specific work as a function of the initial compression temperature for a single stage ammonia compressor between evaporating and condensing temperatures of -23.3°C and 54.4°C, respectively. In this case, the specific work increases by 23% if the initial compression temperature changes from -10ºC to 50°C. Also shown in Fig. 1 is the ammonia mass flow rate, which has been normalized with respect to the mass flow rate corresponding to an initial compression temperature of -10ºC. Accordingly, a 20% decrease in the mass flow rate is verified when the initial temperature is 50°C.

An important heat transfer aspect of ammonia refrigeration systems is that liquid-suction heat exchangers are usually avoided in order to prevent a further decrease in the system efficiency due to inlet gas superheating. Hence, the refrigerant temperature in the compressor suction system has a comparatively lower value, which enhances the heat transfer to the refrigerant along its path to the suction valve. Therefore, any alternative to reduce the compressor thermal profile as a whole will have a great impact on the system efficiency. In Fig. 2, a comparison between the isentropic and isothermal compression processes is represented in a pressure-normalized volume (P-$\bar{V}$) diagram for a single stage (-23.3°C, 54.4°C) ammonia compressor with an initial compression temperature of 60ºC. As can be seen, the isothermal compression requires much less compression work than the isentropic compression for a given pressure ratio. At the present condition, the specific work in the isothermal compression is 28.9% less than the isentropic one. Naturally, an isothermal compression is extremely difficult to be achieved in practice due to the extremely high heat fluxes required. Additionally, the refrigerant temperature is limited by the temperature of the

external environment, unless some extra work is added to the process. If the initial compression temperature is lower than the temperature of the external environment, the best alternative would be to start the compression process as isentropic and, after reaching the condensing temperature, follow an isothermal compression.

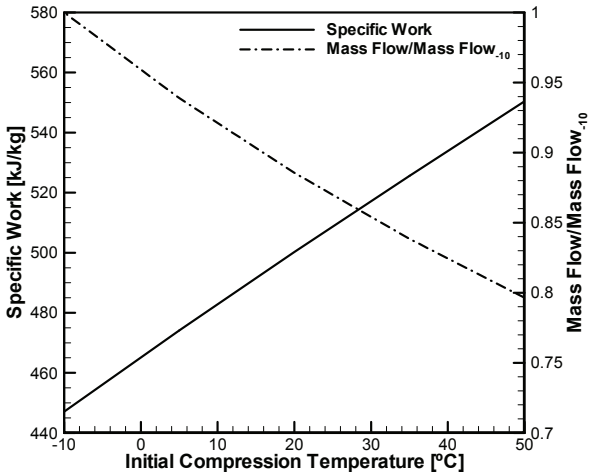

Figure 1: Effect of superheating.

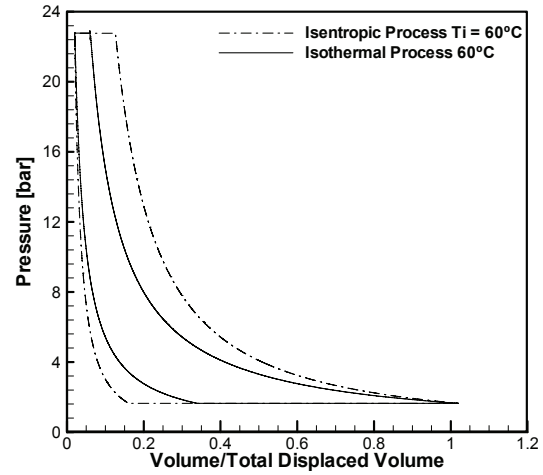

Figure 2: Effect of compression process.

Compressor cooling as a means of reducing the compression power has received some attention in the literature in the past few years. Dutta *et al.* (2001) investigated theoretically and experimentally the effect of liquid refrigerant injection in scroll compressors using R-22. A decrease in the vapor temperature during compression was observed. However, the extra work required to compress the vaporized refrigerant gave rise to a decrease in the compressor performance. The experimental and numerical studies of Coney *et al.* (2002) quantified the decrease in power consumption (approximately 28%) associated with the atomization of water in air reciprocating compressors. Meunier (2006) conceived a refrigeration cycle with a COP equal to that of the Carnot refrigerator in which superheated vapor is compressed isothermally. Bonjour and Bejan (2006) demonstrated that the existence of an optimal configuration for the distribution of cooling water in a multi-stage ammonia compressor which minimizes the compressor power. Additionally, it was shown that for a given refrigerant mass flow rate, the optimal coolant mass flow rate is insensitive to the isentropic efficiency. Wang *et al.* (2007) investigated theoretically two performance improving options to reduce the compressor power for several refrigerants. The first option was to cool the motor by external means other than using the suction gas. The second was to combine the processes of isothermal and isentropic compression. The analysis demonstrated that the first option is more advantageous for LBP rather than HBP applications for all refrigerants investigated. The second option showed that the compression power can be reduced by up to about 16% depending on operating conditions and working fluid.

In the present paper, the thermal effect of atomization of lubricant oil (ISO 10) is theoretically investigated during the compression of ammonia in a reciprocating compressor. Oil atomization increases the heat transfer surface inside the cylinder, thus enhancing significantly the heat removal from the vapor as it is compressed. The resulting cooling effect also contributes to lowering the overall thermal profile of the compressor parts and, consequently, the initial compression temperature. Nevertheless, this second beneficial effect will not be considered in the present study.

2. MATHEMATICAL MODELLING

2.1 In-cylinder Gas Compression

The control volume formulation of the vapor compression process is based on the work of Ussyk (1984). The mass and energy conservation equations for the vapor are given by

$$\frac{dm}{dt} = \sum \dot{m} = \dot{m}_s - \dot{m}_d - \dot{m}_l - \dot{m}_{sr} + \dot{m}_{dr} \tag{1}$$

$$m\frac{du}{dt} = \dot{Q}_o + \hbar A_w\left(T_w - T\right) - p\frac{d\mathcal{V}}{dt} - u\frac{dm}{dt} - \sum \dot{m}h \tag{2}$$

where $u = u\left(p,T\right)$ is the internal energy of the vapor. Additional relationships for the pressure and enthalpy fluxes are as follows

$$p = \frac{m}{\mathcal{V}} Z\Re T \tag{3}$$

$$\sum \dot{m}h = \left(\dot{m}_d + \dot{m}_l + \dot{m}_{sr}\right)h - \dot{m}_s h_{sc} - \dot{m}_{dr} h_{dc} \tag{4}$$

In the present work, the cylinder is considered adiabatic ($\hbar$ = 0). The physical properties of the refrigerant were calculated from REFPROP 7.0 (Lemmon *et al.*, 2002).

2.2 Droplet Atomization and Heat Transfer

The compression cycle is divided into n time steps of size Δt. The number of spherical droplets injected into the cylinder in a given time step is given by

$$N = \frac{3\dot{V}_o \Delta t}{4\pi R^3} \tag{5}$$

In the following analysis, the subscripts m,n (as in $N_{m,n}$) denote the group of droplets that were injected into the cylinder at a given instant m and still are in the cylinder at an instant $n > m$. It is assumed that all droplets in each group m are identical with respect to their size, velocity and temperature. If coalescence, break-up and evaporation are neglected, mass conservation for each group m gives

$$\frac{dN_{m,n}}{dt} = -\frac{\dot{M}_{m,n}}{M_m} \tag{6}$$

The mass flow rate of droplets of a group m through the discharge valve is calculated based on their mass fraction in the cylinder, $x_{m,n}$, as follows

$$\dot{M}_{m,n} = F\, x_{m,n}\, \dot{m}_t \tag{7}$$

where

$$x_{m,n} = \frac{N_{m,n} M_m}{m + \sum_{m=0}^{n} N_{m,n} M_m} \tag{8}$$

and F is a droplet discharge slip factor that accounts for the relative velocity between vapor and liquid in the discharge stream. When F = 1 (homogeneous flow), the dynamic mass fraction of droplets during discharge is equal to their in-cylinder mass fraction. In this analysis, a value of F equal to 0.65 was obtained from a numerical simulation of the atomization process inside the cylinder, as detailed in Kremer *et al.* (2007). The gas mass flow rate through the discharge valve is given by

$$\dot{m}_d = \left(1 - F\, x_{m,n}\right)\dot{m}_t \tag{9}$$

Due to the presence of droplets in the cylinder, a correction is applied to the instantaneous cylinder volume to obtain the vapor volume

$$\mathcal{V} = \mathcal{V}_c - \frac{4\pi}{3}\sum_{m=0}^{n} N_{m,n} R_m^3 \tag{10}$$

$$\frac{d\mathcal{V}}{dt} = \frac{d\mathcal{V}_c}{dt} - \frac{4\pi}{3}\sum_{m=0}^{n} R_m^3 \frac{dN_{m,n}}{dt} \tag{11}$$

where $\mathcal{V}_c$ and its time derivative are calculated from algebraic relationships for the piston position and velocity as a function of the crankshaft angle (Ussyk, 1984).

The velocity of the oil droplets is calculated from Newton's Second Law. Neglecting the effect of body forces, assuming that the velocities of the droplets are much larger than the in-cylinder vapor velocity and that the hydrodynamic interaction between neighbouring droplets is small, one has

$$\frac{dU_{m,n}}{dt} = \frac{3\rho C_D U_{m,n}^2}{8\rho_o R_m} \tag{12}$$

where C_D is the drag coefficient calculated from the Morsi and Alexander (1972) correlation. The average droplet radius, R_m, was found to be 0.7 µm (Kremer *et al.*, 2007). The initial condition for $U_{m,n}$ is calculated from

$$U_{n,n} = C_d\sqrt{2(p_C - p)/\rho_o} \tag{13}$$

where C_d is the nozzle discharge coefficient, assumed equal to 0.78 (Lichtarowicz *et al.*, 1965). In Equation (13), ρ_o is the oil density at the injection temperature. Since the vapor pressure of the oil is small, it is assumed that only sensible heat transfer takes place between the droplets and the vapor. Temperature gradients inside the droplets and thermal interaction between droplets are ignored. Thus, the temperature of a droplet in group m at an instant n is calculated from

$$\frac{dT_{m,n}}{dt} = \frac{3h_{m,n}}{\rho_o c_{po} R_m}\left(T - T_{m,n}\right) \tag{14}$$

where the oil physical properties are calculated at the mixing-cup temperature of the droplets in the cylinder. $h_{m,n}$ is the heat transfer coefficient between the gas and droplets calculated from the Ranz and Marshall (1952) correlation. The heat transfer rate between all oil droplets and the vapor is given by

$$\dot{Q}_o = 4\pi R_m^2 \sum_{m=0}^{n} N_{m,n} h_{m,n}\left(T_{m,n} - T\right) \tag{15}$$

It is further assumed that heat removal from the cylinder wall by the droplets is small and can be neglected. Droplets that remain in the clearance volume at the end of a compression cycle are assumed to have, in the next cycle, zero initial velocity and initial temperature equal to that of the vapor.

The resulting cooling effect on the overall thermal profile of the compressor was not considered in the present simulations. Therefore, the benefits associated with thermal originated by the oil atomization in the cylinder will be probably greater than that observed in the present analysis.

2.3 Suction and Discharge Processes

Valve displacement during suction and discharge is calculated via a one-degree-of-freedom model with natural frequency and damping coefficients specific for each valve. The resultant forces on the valves and their respective flow rates are obtained with effective force and effective flow areas derived from numerical simulations (Matos, 2002). The total flow rate through the discharge valve is calculated assuming a homogeneous two-phase density based on the discharge mass fraction of each phase (Equations 7-9).

3. RESULTS

In order to obtain the numerical results, the compression cycle was divided into 10^3 uniform time (or crank angle) steps and an explicit Euler method was used to integrate the time-dependent mass and energy conservation equations for the vapor and droplet fields. The conditions of the simulation reported here are as follows: (i) evaporation and condensation temperatures: -23.3°C and 54.4°C, (ii) refrigerant: ammonia; (ii) vapor temperature entering the cylinder: 32°C; (iii) compressor speed: 60Hz; (iv) compression rate: 42.

The influence of three independent variables has been assessed: (i) the oil injection temperature, which was varied between 30 and 60°C; (ii) the oil atomization flow rate, which was varied between 0.54 and 2.89 times the refrigerant mass flow rate; and (iii) the nozzle position relative to the valve plate, *x*, which was varied between 0.11 and 0.84 times the piston stroke, *L* (see Fig. 3).

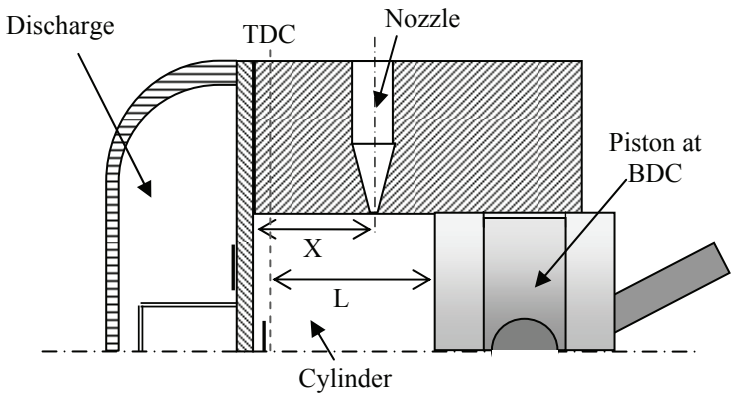

Figure 3: Schematic of the nozzle positioning.

Figure 4 shows the transfer of heat from the vapor as a function of the crank angle for the atomization of oil at 54°C, with an oil-to-ammonia mass flow ratio ($\dot{M}_{oil}/\dot{M}_{ammonia}$) of 1.10 and normalized nozzle position of 0.68. In the atomization case, heat transfer during compression increases more sharply and becomes positive earlier in the cycle showing a strong influence of droplet heat transfer. During expansion, heat transfer is almost zero as a result of the very low velocity of the droplets remaining in the clearance volume after discharge. In Fig. 5, *TV* diagrams reveal a significant reduction of the vapor temperature (as high as of 80°C at the TDC). The initial compression temperature keeps almost constant in both cases due to not considering the cooling effects on the overall thermal profile. Figure 6 shows the oil atomization effects on the *PV* diagram. The sharper pressure drop during expansion observed for the oil atomization case can be explained based on the smaller residual volume occupied by the vapor due to the presence of oil in the cylinder when the piston is at the TDC. This effect seems to be more important than that associated with the lower final compression in determining the crank angle at which the suction valve will open. Figure 7 shows the path of the refrigerant in the compression process in a *T-s* diagram. In the oil atomization case the compressor process has a significant change, but it is still quite far from the isothermal compression.

The effect of nozzle location inside the cylinder is investigated in Table 1. The nozzle is assumed to be mounted flush on the cylinder wall and its normalized position is defined based on piston stroke. Depending on the nozzle position, the orifice remains covered for a certain region of the cycle (before and after the TDC) and no droplet atomization takes place during this period. The temperature with which the oil enters the compressor is maintained at 54°C in all cases.

As expected, for smaller distances between the orifice and valve plate, more oil enters the cylinder per cycle but no significant differences were found in the specific effective work (w_{ef}). The normalized mass flow rate ($\dot{M}/\dot{M}_{Baseline}$) reduction with decreasing nozzle position is mainly due to more oil injection during expansion which causes a delay in the opening of the suction valve. The mass flow rate becomes lower than the baseline case when the normalized position is less than 0.53. Although no differences were found in w_{ef}, the w_{pv} work increases for smaller distances between the nozzle orifice and valve plate due to an increase in the losses associated with the discharge process.

The effect of oil flow rate for a fixed normalized nozzle position (0.68) and oil temperature (54°C) is seen in Table 2. This was achieved using a multiplying factor for the oil flow rate in Equation (5). The mass flow rate decrease with the oil flow rate and becomes lower than the baseline case for values of $\dot{M}_{oil}/\dot{M}_{ammonia}$ greater than 1.70. The specific effective work decreases with the oil flow rate as result of the significant increase of the net specific heat capacity, q_{net} (energy transferred per kilograms of ammonia). The difference between w_{ef} can reach up to 4.2% compared with the baseline. It is worth mentioning that, if the effects of the compression cooling on the overall compressor profile are incorporated into the analysis, a more substantial gain could have been achieved. Additionally, special attention should be paid to the discharge system in order to reduce the losses in this region resulting from the increase of the oil flow rate being discharged from the compressor.

The effect of the oil temperature entering the injection line for a fixed position ratio (0.68) and a fixed flow rate ($\dot{M}_{oil}/\dot{M}_{ammonia}$ = 1.10) is depicted in Table 3. As can be seen, the droplet-vapor heat transfer potential is inversely proportional to the oil temperature. Moreover, higher oil temperatures also increase the effective specific work. Difference in w_{ef} reaches up to 5.3% for oil injection at 30ºC, but considering that the condensing temperature is 54.4ºC it is very unlikely that such low temperatures can be achieved in practice.

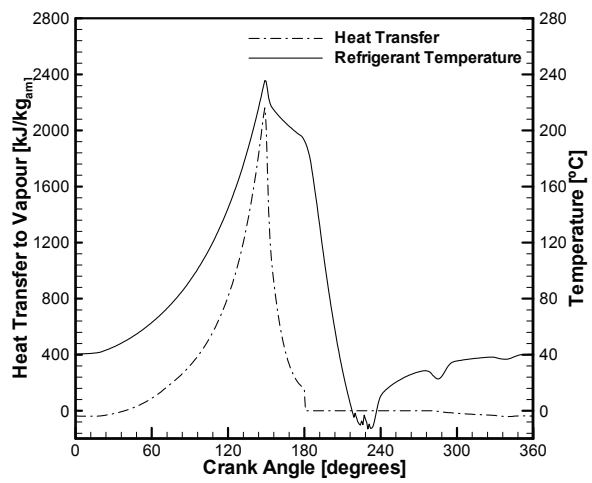

Figure 4. Heat transfer as a function of crank angle.

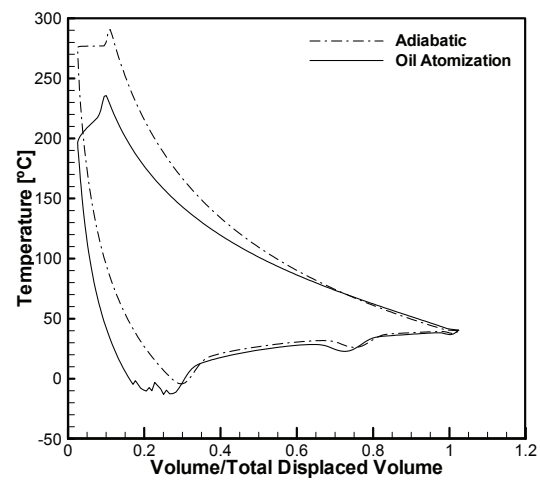

Figure 5. *TV* behaviour of refrigerant vapor.

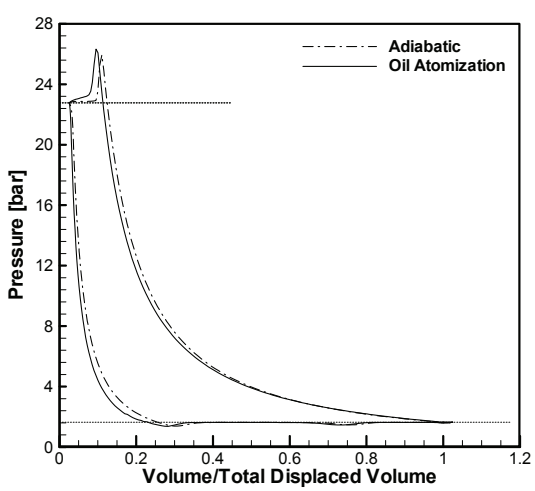

Figure 6. Effect on *PV* diagram.

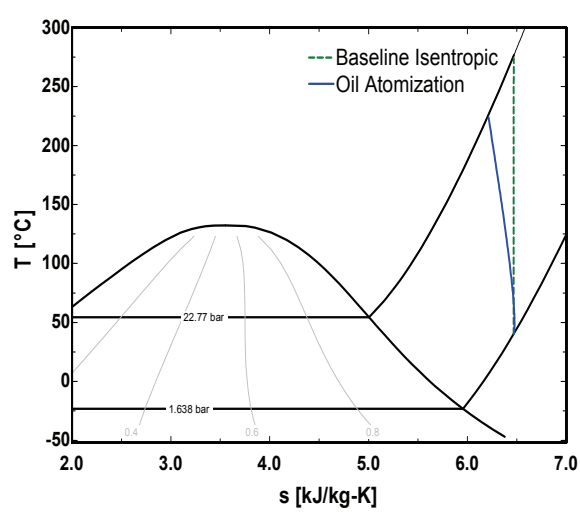

Figure 7. T-s diagram.

Table 1. Effect of nozzle location.

	Baseline	Nozzle position – Position/Stroke					
		0.11	0.21	0.37	0.53	0.68	0.84
$M_{oil}/M_{Ammonia}$	0.000	2.187	1.969	1.676	1.396	1.099	0.759
q_{net} [kJ/kg]	0.0	348.5	328.1	297.0	262.0	218.3	165.7
w_{pv} [kJ/kg]	577.8	570.0	568.6	567.7	566.7	564.6	566.6
w_{ef} [kJ/kg]	565.3	549.2	548.9	549.4	549.5	548.6	551.7
$\dot{M}/\dot{M}_{Baseline}$	1.000	0.978	0.984	0.995	1.008	1.027	1.034
Diff. w_{ef} [%]	**0.00**	**-2.85**	**-2.90**	**-2.82**	**-2.80**	**-2.95**	**-2.40**

Table 2. Effect of oil atomization flow rate.

	Oil Flow Rate					
$M_{oil}/M_{Ammonia}$	Baseline	0.54	1.10	1.70	2.30	2.89
q_{net} [kJ/kg]	0.0	123.0	218.3	297.8	363.0	411.2
w_{pv} [kJ/kg]	577.8	564.9	564.6	566.7	567.7	566.0
w_{ef} [kJ/kg]	565.3	550.9	548.6	548.1	546.3	541.5
$\dot{M}/\dot{M}_{Baseline}$	1.000	1.045	1.027	0.997	0.975	0.969
Diff. w_{ef} [%]	**0.00**	**-2.55**	**-2.95**	**-3.04**	**-3.36**	**-4.20**

Table 3. Effect of oil temperature.

	Baseline	Oil Temperature in Suction Chamber [ºC]					
		30	36	42	48	54	60
q_{net} [kJ/kg]	0.0	242.9	238.1	233.0	226.7	218.3	212.6
w_{pv} [kJ/kg]	577.8	551.3	555.4	559.3	562.0	564.6	567.6
w_{ef} [kJ/kg]	565.3	535.4	539.4	543.3	546.0	548.6	551.5
$\dot{M}/\dot{M}_{Baseline}$	1.000	1.032	1.028	1.024	1.025	1.027	1.027
Diff. w_{ef} [%]	**0.00**	**-5.29**	**-4.58**	**-3.90**	**-3.41**	**-2.95**	**-2.44**

4. CONCLUSIONS

A comprehensive model was presented to evaluate the effect of in-cylinder oil atomization in reciprocating ammonia compressors. The influence of several parameters such as oil injection temperature, nozzle position and oil mass flow rate was investigated. A normalized nozzle position of 0.68 has presented the best compromise between a reduction of the specific compression work with the lowest oil injection flow rate. By increasing the atomization flow rate, it was shown that the energy consumption can be reduced by as much as 4.2%. Despite the significant reduction of the specific compression work due to the injection of oil at a low temperature, it is unlikely that, in practice, this could be achieved for oil injection temperatures below the condensing temperatures without an external cold source.

NOMENCLATURE

h	specific enthalpy (kJ/kg)	T	temperature (^{o}C)	l	leakage
$\bar{h}$	heat transfer coefficient (W/m^{2}K)	$\dot{V}$	volume flow rate (m^3/s)	o	oil
m	mass of vapor (kg)			r	reflux
M	mass of a single oil droplet (kg)	**Subscripts**		s	suction
$\dot{m}$	mass flow rate of vapor (kg/s)	C	condensation	t	total
$\dot{M}$	mass flow rate of droplets (kg/s)	d	discharge	w	wall

REFERENCES

Bonjour, J., Bejan, A., 2006, Optimal distribution of cooling during gas compression, *Energy*, 31, pp. 409-424.

Coney, M.W., Stephenson, P., Malmgren, A., Linnemann, C., Morgan, R.E., Richards, R.A., Huxley, R., Abdallah, H., 2002, Development of a reciprocating compressor using water injection to achieve quasi-isothermal compression, *Proc. 16th Int. Compressor Engineering Conference at Purdue*, CD-ROM.

Dutta, A.K., Yanagisawa, T., Fukuta, M., 2001, An investigation of the performance of a scroll compressor under liquid refrigerant injection, *Int. J. Refrig.*, 24, pp. 577-587.

FLUENT 6.2.16, 2005, User Manual, Fluent Inc.

Gosney, W.B., 1982, *Principles of Refrigeration*, Cambridge University Press.

Kremer, R., Barbosa, Jr., J.R., Deschamps, C.J., 2007, Theoretical analysis of the effect of oil atomization in the cylinder of a reciprocating compressor, *Int. Conf. on Compressors and their Systems*, London, paper C658-039.

Lemmon, E.L., McLinden, M.O., Huber, M.L., 2002, REFPROP 7.0, NIST, USA.

Lichtarowicz, A.K., Duggins, R.K., Markland, E., 1965, Discharge coefficients for incompressible non-cavitating flow through long orifices, *J. Mech. Engng. Sci.*, v. 7, p. 2.

Matos, F.F.S., 2002, Numerical Analysis of the dynamic behavior of reed-type valves of reciprocating compressors, Ph.D. Thesis, Federal University of Santa Catarina (in Portuguese).

Meunier, F., 2006, Refrigeration Carnot-type cycle based on isothermal vapour compression. *Int. J. Refrig.,* v. 29, pp. 155-158.

Morsi, S.A., Alexander, A.J., 1972, An investigation of particle trajectories in two-phase flow systems, *J. Fluid Mech*., v. 55, pp. 193-208.

Ranz, W.E., Marshall, W.R., 1952, Evaporation from drops – I and II, *Chem. Eng. Prog*., v. 48, pages 141, 173.

Ussyk, M.S., 1984, Numerical simulation of hermetic reciprocating compressors, M.Eng. Diss., Federal University of Santa Catarina (in Portuguese).

Wang, X., Hwang, Y., Radermacher, R., 2007, Investigation of potential benefits of compressor cooling, *Applied Thermal Engineering*, in press.

ACKNOWLEDGEMENTS

The material presented in this paper is a result of long-standing technical-scientific partnership between the Federal University of Santa Catarina (UFSC) and Embraco. Support from FINEP, CNPq and CAPES is also acknowledged.